

# Miniaturized high-performance MEMS accelerometer detector

Stephan Gonseth<sup>1</sup> · Felix Rudolf<sup>1</sup> · Christoph Eichenberger<sup>2</sup> · Dick Durrant<sup>3</sup> · Phil Airey<sup>4</sup>

Received: 27 October 2014 / Revised: 23 April 2015 / Accepted: 24 April 2015 / Published online: 6 May 2015  
© CEAS 2015

**Abstract** In the framework of the demonstration of European capabilities for future space exploration mission, a high-performance miniaturized MEMS accelerometer detector is developed by Colibrys for incorporation into a compact inertial measurement unit (IMU). The envisaged missions where a miniaturized IMU is under development by SEA should cover:

- Aerobraking;
- Entry, descent, and landing (EDL); and
- Planetary rovers navigation.

The accelerometer specifications were defined through an ESA study by providing accelerometer component as well as system level requirements for most future planetary application. Based on these needs, the feasibility of a MEMS, high accuracy, low power and miniaturized accelerometer has been successfully demonstrated with an available sensor designed for the aerospace market. The development toward TRL5 of a RadHard MEMS accelerometer is led by Colibrys, and will be made available on the open market for incorporation into IMU and standalone one and three axis accelerometer devices. This activity covers the

development of the radiation hardened ASIC managed by our partner HMT, the design of a fully hermetic ceramic package and a full characterisation test of the accelerometer component. The key parameters are

- Analogue outputs (acceleration and temperature),
- 2 independent accelerometers ( $\pm 1$ ,  $\pm 20$  g) in the same package,
- White noise:  $5 \mu\text{g}/\sqrt{\text{Hz}}$  (1 g sensor),
- Power supply 3.3 V/power consumption per channel: 10 mW,
- Non-linearity: 0.5 %/bandwidth: DC to min 50 Hz and
- 50 krad radiation tolerance

This paper presents the accelerometer performance, lifetime, and environmental requirements. The on-going accelerometer component design and technology will be presented as well as the planned accelerometer testing. The results of a preliminary radiation test single event effects (SEE) and total ionizing dose (TID) performed on a test chip ASIC will be discussed, and the select ASIC architecture with digital redundancy will be shown.

**Keywords** MEMS · Accelerometer · Inertial measurement unit (IMU) · Navigation · Entry, descent and landing (EDL)

---

This paper is based on a presentation at the 9th International Conference on Guidance, Navigation and Control Systems, June 2–6, 2014, Porto, Portugal.

---

✉ Stephan Gonseth  
stephan.gonseth@colibrys.com

<sup>1</sup> Colibrys Ltd, Yverdon-Les-Bains, Switzerland

<sup>2</sup> HMT, Biel/Bienne, Switzerland

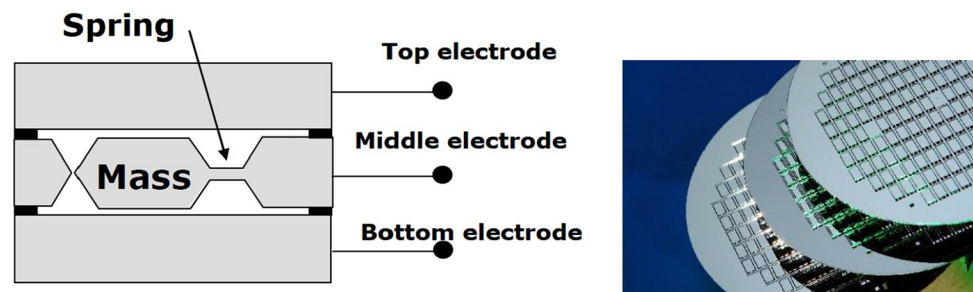
<sup>3</sup> SEA, West Midlands, UK

<sup>4</sup> ESA, Marum, Netherlands

## 1 Introduction

Micro electrical mechanical system (MEMS) accelerometers have been developed at Colibrys since more than 20 years for industrial, military, aeronautic, and safety applications. These sensors have proven high reliability [1, 2] under aggressive environments like firing shocks of

**Fig. 1** MEMS capacitive accelerometer cross section. An out of plane acceleration will deflect the proof mass and change the capacitances between the *middle* and the *top* and *bottom* plate, respectively



20,000 g when used in guided munitions, full operation in drilling application at high temperature and in the presence of heavy vibrations or aggressive environments with repetitive shocks in automotive testing and train bogie monitoring. The robustness of this technology to harsh environment, the full performance over operational temperature and the entire lifetime (up to 10 years), the low power consumption, and the small size factor are key features of MEMS accelerometers. A platform of industrial accelerometer sensors has been developed and qualified to meet the requirements of inertial navigation, tilt measurement for platform stabilization, automotive testing, military guidance and vibration-monitoring applications.

The aim of this work is to develop an accelerometer to address the specific space requirements and especially the immunity against radiation effects such as radiation-induced upsets single event upset (SEU)/multiple bit upsets (MBU) and large total doses. The RadHard accelerometer will be derived from the robust industrial accelerometer platform and requires the hardening of the industrial ASIC.

There are basically two ways of measuring the acceleration with a MEMS sensor: either open or closed loop. In an open-loop configuration, the capacitance change in the MEMS is measured and amplified. In closed-loop electronics, the inertial forces are compensated by electrostatic forces [3]. Closed-loop system allows reaching better ultimate performance in terms of bias stability, linearity and noise. The price to be paid for these ultimate performances is in terms of power (needs very precise high voltage), size (driven by the power supply requirements), and complexity (analogue and digital electronics). For this work, open-loop configuration has been chosen. As compared to closed-loop systems, it has a tenfold advantage in power, size and is significantly less complex, while still reaching the performance required for the space applications.

## 2 Design

Key requirements for high performance and high reliability in harsh environments are a stable mechanical sensor that is a MEMS device and its associated die attach technology.

For the MEMS sensor, a proven capacitive accelerometer qualified in Mil/Aerospace products and based on a bulk micromachining technology is used as illustrated in Fig. 1. It is based on a bulk silicon proof mass suspended by a spring and detecting acceleration in the out of plane direction. It has already shown that excellent performance can be reached with this approach [2]. A new die attach technology was developed with high robustness to repetitive shock and has still minimal die attach stress.

The second key element is the design of the electronics for operation in various environmental conditions, i.e., over the full temperature range and under radiation. In a first phase, an ASIC was designed for industrial applications, including operation at high temperature (175 °C). The capacitive signal from the MEMS sensor is measured by the differential charge balancing loop block. In a control loop, the capacitor bridge is balanced. This concept [4] has already been successfully used in a previous ASIC used in current Colibrys products. In order to improve stability and noise, a fully differential configuration is used providing a positive and negative output signal, the acceleration signal being the difference between the two signals.

The RadHard ASIC is designed with exactly the same analogue chain composed of the MEMS accelerometer, the charge balancing loop (CBL), a programmable gain amplifier (PGA) and a low pass filter (LPF). The remaining digital blocks have them been designed with hardening techniques and redundancy architecture implemented in the nonvolatile memory. The block schematic of the RadHard ASIC is shown in Fig. 2.

The charge balancing loop includes also features to adjust the linearity caused by stray capacitances and sensor nonlinearity. A significant advantage of this concept is that the electrostatic forces applied on either side of the proof mass are always equal, independently of the plate position. This significantly reduces measurement errors caused by electrostatic forces especially for low g accelerometers. The signal from the charge balancing loop is fed through a programmable amplifier and a programmable low pass filter, to provide an easy to use output voltage to the user. The differential output assures that zero g corresponds to positive and negative output being equal, independently of any

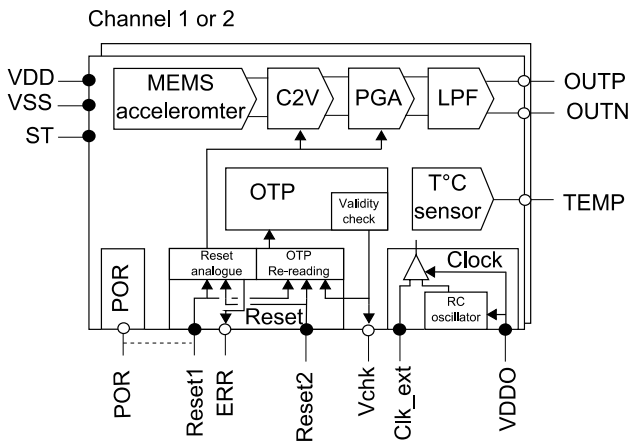


**Fig. 2** Bloc schematic of the RadHard ASIC (both channel are fully independent)

reference voltage. The gain is ratiometric to the power supply voltage i.e., if the power supply is used as a reference for the subsequent A/D converter the accelerometer output becomes largely independent of any power supply voltage variation.

The service blocks include a programmable memory to store the calibration data, an RC oscillator (clock), a power management function (POR) and a reset block (reset). The clock can be generated internally by the RC oscillator when powered or externally through the CLK\_ext pin (in this case, the internal RC oscillator must be grounded). The serial interface is only used in manufacturing to write the calibration data in the OTP memories and is not powered in operation. The ASIC is designed to operate between  $-55$  and  $175$  °C and includes a temperature sensor that can be used for temperature correction by the user. The ASIC operates at 3.3 V, and uses less than 10 mW per channel.

The radiation hard version of the ASIC integrates the industrial analogue chain circuit, uses the same technology and is designed for immunity against radiation (SEU/MBU) and for a total dose of 50 krad. All the digital blocks have been redesigned using hardening technics including pseudo-ELT transistors, deep trench isolation and guard ring. Furthermore, triple redundancy voting is implemented to guarantee that the configuration and calibration data are valid. In case of a single or multiple set-ups (SEU/MBU), the data are refreshed from the one time programmable (OTP) memory to correct the errors. This is done in the background, without affecting the operation of the analogue signal chain.

The RadHard accelerometer SA0120 (Fig. 3) consists of two capacitive MEMS accelerometers and their associated ASIC electronics, hermetically sealed in the same ceramic package. Each accelerometer has a dual voltage differential output proportional to the acceleration and one voltage temperature output proportional to the temperature. Enhanced performance can be achieved through an external mathematical modelling of the bias, scale factor and axis misalignment over temperature that can be referenced to the supplied temperature output.

The target accelerometer and electrical performances as well as the environment specifications have been defined in an initial study [5] and are expressed in the following Tables 1, 2 and 3.

### 3 Accelerometer manufacturing and testing

The prototypes manufactured and characterized in this phase are based on the industrial ASIC which share a common analogue chain with the RadHard version currently in development. The same assembly technology and MEMS

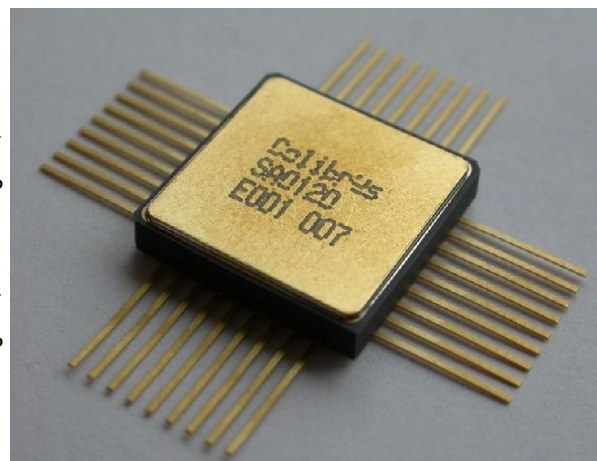
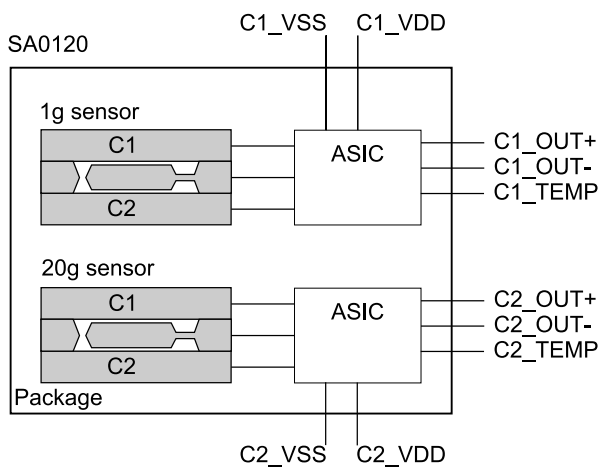


**Fig. 3** SA0120 dual range accelerometer schematic (left) and SA0120.a product (right)

**Table 1** Target accelerometer performances

	Units	1 g sensor	20 g sensor
Full-scale range	g	$\pm 1$ g	$\pm 20$ g
Bias calibration	mg, $1\sigma$	<1	<20
Bias stability (1 h)	mg, $1\sigma$	0.025	0.050
Bias stability (24 h)	mg, $1\sigma$	0.050	0.100
Scale factor sensitivity (K1)	mV/g	2700	135
Scale factor stability	ppm $1\sigma$	300	300
Input axis misalignment (Kp, Ko)	mrad, $1\sigma$	17.5	17.5
One year axis misalignment stability	$\mu$ rad, $1\sigma$	300	300
Non-linearity	% of FS max.	<0.5	<0.5
Bandwidth	Hz	0 to $\geq 50$	0 to $\geq 50$
Noise spectral density in band	$\mu$ g/ $\sqrt{\text{Hz}}$ max.	5	100
Vibration rectification error	$\mu$ g/g <sup>2</sup>	–	50

accelerometer are used and the performances can be directly extrapolated to the RadHard product. The results presented in this chapter have been measured on an industrial accelerometer (Fig. 4).

The prototypes use a new die attach technology to make them very robust to shock and temperature variation. This technology as well as the MEMS accelerometer sensor is already integrated in the existing Colibrys RS9000 product family that serves as the test vehicle. Shock test was performed on the RS9010.b devices (10 g device) to qualify the technology: one with multiple shocks of low amplitude and one with multiple shocks of high amplitude.

The low amplitude shock test consisted of 20 shocks of 740 g. These tests were performed at  $-30$ ,  $20$ ,  $80$  °C, on 14

accelerometers. The measured bias shift was <44 ppmFS. This die attach technology is also applied for the new generation of accelerometers. The ppm of full scale (ppmFS) unit is used in this document for different measurements in order to be able to extrapolate rapidly the performance to the 1 g or the 20 g sensors.

The high shock test consisted of 90 shocks of 6000 g, 0.15 ms. Tests were performed on 13 samples. No sample failed. Figure 5 shows the variation of bias during these tests. The maximum observed bias shift was 1250 ppmFS and the sensitivity shift >400 ppm. As a comparison, devices with the previous die attach technology would generally fail under these conditions.

The calibration of the non-linearity is a critical step during manufacturing at Colibrys. The charge balancing loop has two parameters to adjust the even and odd nonlinearity components independently. A calibration method based on the IEEE std 1293-1998 [6] is performed on a shaker. This method is based on a fitting of the response curve with a 6th order polynomial and subtracting the constant term (bias) and the first-order term (sensitivity). The calibration is done against a piezoelectric reference accelerometer. This is clearly a limitation since the nonlinearity of the reference accelerometer is of the same order as the nonlinearity goal of the accelerometer to be tested. Typical non-linearity curves of calibrated accelerometers are shown in Fig. 6.

The long-term behaviour was assessed by measuring the bias shift over a period of >55 h powered at 85 °C. This corresponds roughly to 2 years of lifetime at room temperature assuming an electronic standard activation energy of 0.8 eV. As seen in Fig. 7, the bias drift over a long-time duration is less than 100 ppmFS.

**Table 2** Electrical performances

Input voltage (VDD–VSS)	3.0–3.6 VDC. The standard voltage for calibration is 3.3 VDC
Output voltage range	$\pm 2.7$ V (differential output)
Operating current consumption	<3 mA @ 3.3 VDC (per channel)
Output impedance/load on OUP, OUTN, TEMP	Min. 100 k $\Omega$ Max. 100 pF

**Table 3** Target environmental specifications

Operating temperature range	$-40$ to $+80$ °C
Non-operating temperature range	$-60$ to $+120$ °C
Total ionizing dose	>50 krad
Single event latch-up	Immune to single event latch-ups for a linear transfer of up to 80 MeV cm <sup>2</sup> /mg
Single event upset	Immune to single event upset for up to 60 MeV cm <sup>2</sup> /mg
Single event transients	Immune to single event transient for up to 60 MeV cm <sup>2</sup> /mg
Shock resistance	Up to 1000 g/0.66 ms (half-sine, along any axis)
Vibration	20 g rms, 20–2000 Hz (random noise, 30 min in each direction <i>o</i> , <i>p</i> , <i>i</i> )

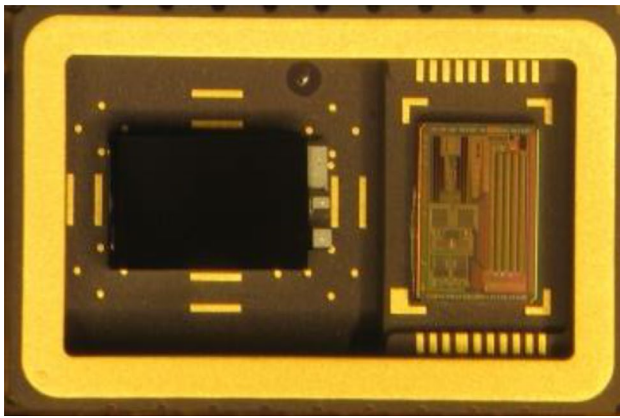


**Fig. 4** Industrial accelerometer prototype with the MEMS (left) and the ASIC (right) in a hermetically sealed ceramic housing

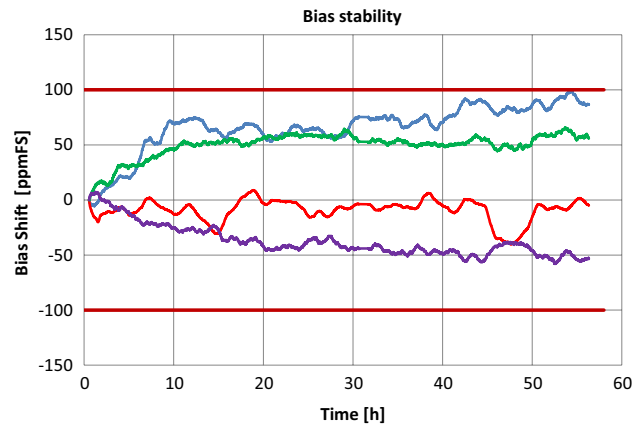


**Fig. 7** Bias drift measured at 85 °C over >55 h. The four curves are from four different devices

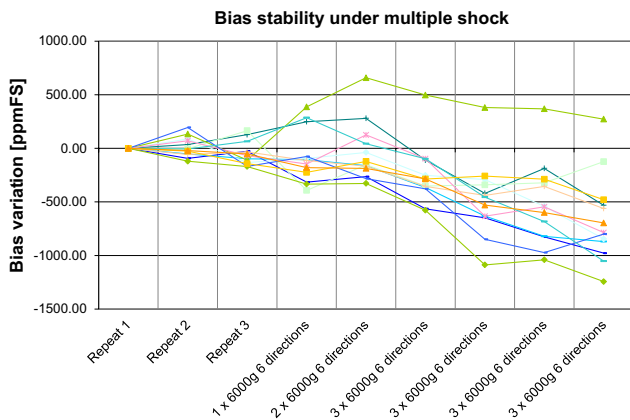


**Fig. 5** Evolution of bias during the multiple shock tests

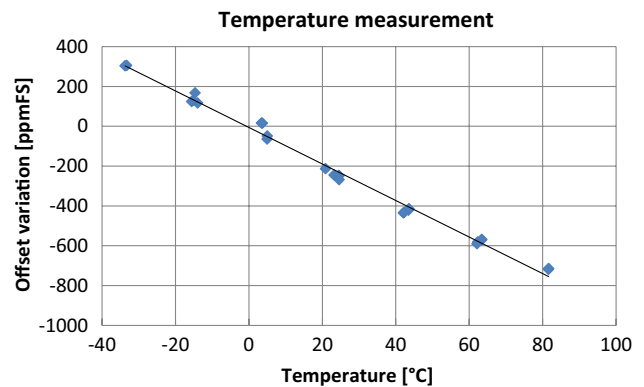


**Fig. 8** Bias shift over temperature

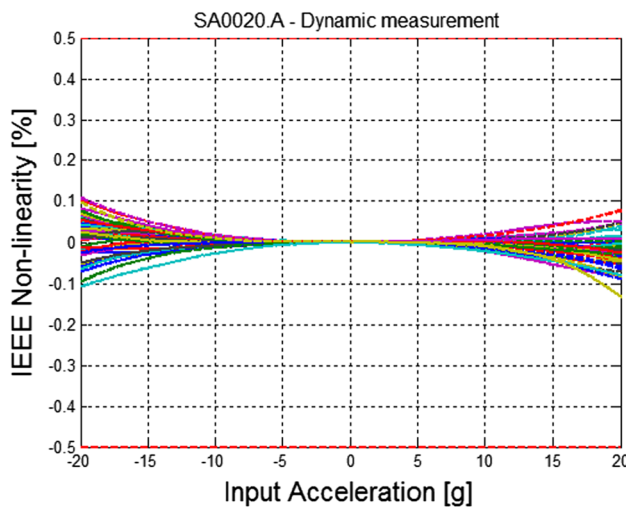


**Fig. 6** SA0120 nonlinearity of calibrated 20 g FS sensor

Figure 8 shows the temperature dependency of bias with a preliminary assessment of the temperature behaviour. The curves represent data points measured over two temperature cycles 20→80→−30→20 °C. The offset temperature coefficient measured on 10 samples is typically −9 ppmFS/°C. The deviation from a straight line fit is <60 ppmFS. This represents the maximum repeatability error caused by temperature hysteresis and possibly measurement errors.

The noise spectrum is shown in Fig. 9. From this graph, we can extract a white noise of 1.7 ppmFS/√Hz and a Flicker noise corner at 0.2 Hz.

Figure 10 shows an Allan Variance plot that is in good agreement with the noise spectrum measurement. The Allan Variance shows that the bias drift due to Flicker noise is below 1 ppmFS.

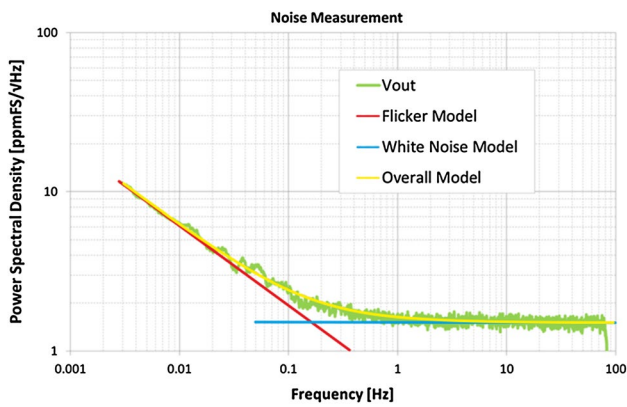


**Fig. 9** Noise spectrum. The data were acquired at 200 Hz with a filter at 90 Hz. The dotted lines show the models for Flicker and white noise

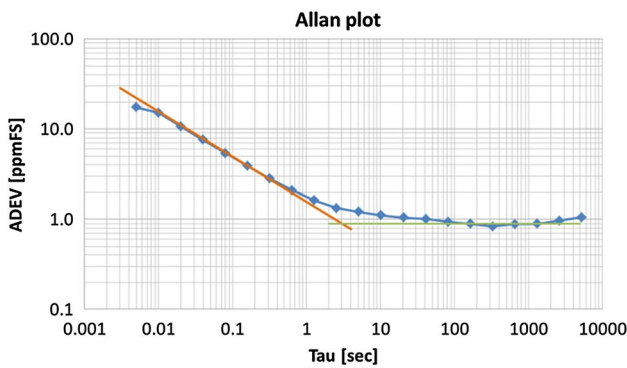


**Fig. 10** Measured allan variance

### 4 Radiation hardening

In order to assess the gap to be closed between the industrial ASIC and a radiation hardened ASIC, a set of tests were performed. Several test structures and an early prototype of the new ASIC not designed for radiation hardness were tested under gamma radiation and were operated under heavy ion bombardment. The goal of the total dose test was to identify any drifts induced by the radiation on the analogue chain. Measurement under heavy ion bombardment allowed to test latch-up immunity of the technology and to evaluate the effect of radiation events on the output signal.

The TID experiment was performed up to a total dose of 54 krad with a Cobalt-60 source and measurement of specific accelerometer performances were performed prior and post radiation. A potential effect of radiation could be a change of the characteristics of the capacitor bank used for non-linearity compensation. The Fig. 11 shows that the non-linearity has not been affected after TID and annealing. In this set-up, the nonlinearity calibration was not optimized

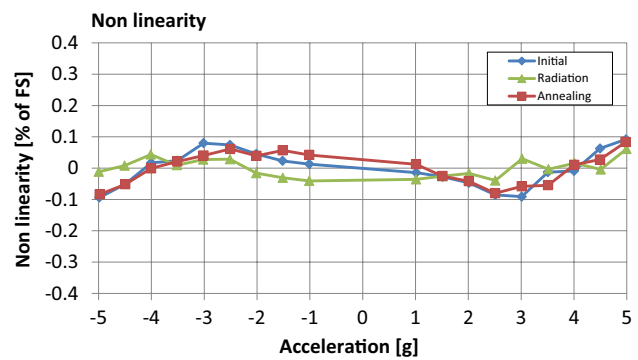


**Fig. 11** Nonlinearity measured before, after radiation and after an annealing step

**Table 4** SEE irradiation steps

	1	2	3	4
ION	$^{40}\text{Ar}^{8+}$	$^{40}\text{Ar}^{8+}$	$^{132}\text{Xe}^{26+}$	$^{132}\text{Xe}^{26+}$
Fluence (particles/cm <sup>2</sup> )	10 <sup>6</sup>	10 <sup>6</sup>	10 <sup>6</sup>	10 <sup>6</sup>
Flux (particles/sec/cm <sup>2</sup> )	3000	3000	3000	3000
Tilt (°)	0	55	0	45
Energy (MeV)	150	150	459	459
LETEFF (MeV/mg/cm <sup>2</sup> (Si))	14.1	24.6	55.9	79
Range (µm)	42	24.1	43	30.4

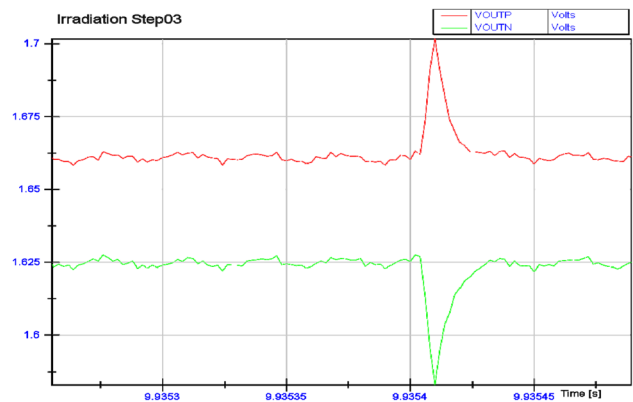


**Fig. 12** Spike observed on the output signal of the ASIC: the top and bottom curves are the positive and negative channel of the differential charge balancing loop bloc

and the measurement accuracy was not sufficient, hence the spread of some of the data points. For this nonlinearity measurement, the straight line fit method was used.

In the heavy ion bombardment experiment, the sensors were operated and exposed to radiation as described in Table 4. The accelerometer differential outputs data were recorded at 500 kHz without filtering so that short spikes events can be easily detected. A typical spike detected in the irradiation step 3 is shown in Fig. 12.

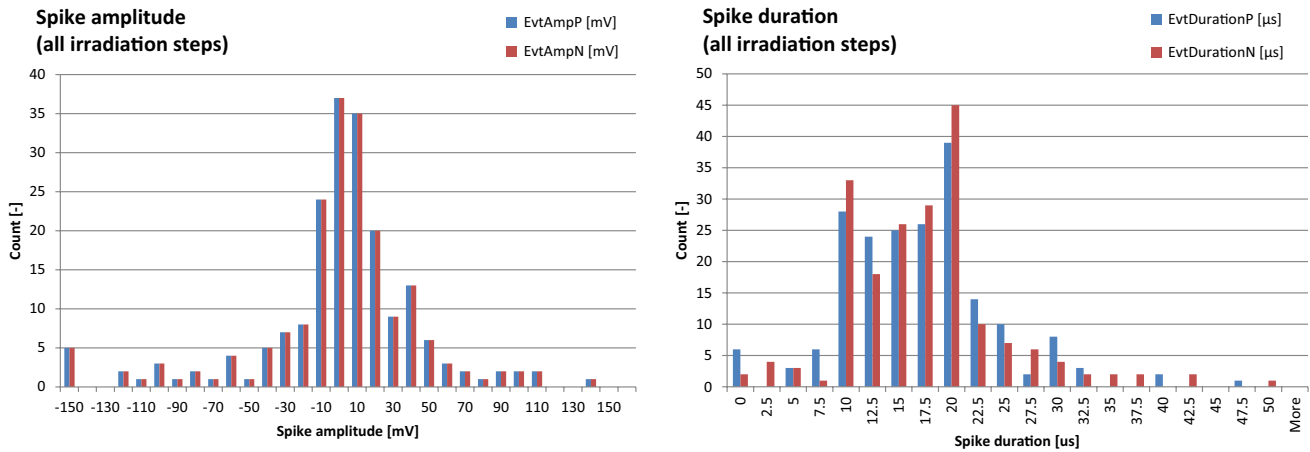


Fig. 13 Spike amplitude (left) and duration (right) for all irradiation steps

The spike amplitude and duration of the four irradiation steps data were extracted and the distribution is shown on Fig. 13. These spikes will appear as signal on the accelerometer output but will be almost completely filtered when passing through the 500 Hz low pass filter of the ASIC (not present in the test chip). The analogue chain was already immune against radiation effects and will be used unchanged in the Radhard ASIC.

We have also identified that the industrial ASIC and the chosen technology is sensitive to SEU and possible to MBU but immune against radiation-induced latch-up. The SEU observed on the digital blocs has led to changes in the sensor calibration which has affected the sensor performance. Therefore, radiation hardening techniques is required on all digital blocks and redundancy implemented in the memory circuit which stores the calibration and configuration data.

### 5 Conclusion

The development of the SA0120 RadHard MEMS accelerometer is led by Colibrys and will be made available on the open market, as a component fully suitable for use in space applications and incorporation into inertial measurement units or for standalone one and three axis accelerometer units.

This product is based on the highly robust industrial technology developed at Colibrys since more than 20 years for industrial, military, aeronautic and safety applications, and has performance, packaging and radiation hardening improvements in order to be compatible with the space environment and application needs. The initial characterization of the latest industrial prototype accelerometers (which now share the same ASIC analogue chain, use the same ASIC technology, MEMS accelerometer and

Table 5 Key target specification and compliance

	Units	1 g sensor		20 g sensor		Test sample
		Target spec	Results	Target spec	Results	
Full-scale range	g	±1 g	±1 g	±20 g	±20 g	Space prototype
Scale factor	mV/g	2700	2700	135	135	Space prototype
Non-linearity, max	% of FS	0.5	0.2	0.5	0.2	Space prototype
Noise spectral density in band, max	µg/√Hz	5	1.7	50	34	Space prototype
Bandwidth, DC to min	Hz	0 to ≥50	0 to ≥100	0 to ≥50	0 to ≥100	Space prototype
Radiation tolerance <sup>a</sup>	Krad	>50	54	50	54	Industrial prototype
Power consumption per channel	mW	10	10	10	10	Space prototype
Mass	g	5				
Size	mm <sup>3</sup>	15 × 15 × 3				

<sup>a</sup> The preliminary radiation results obtained on test chip ASICs have demonstrated the immunity of the analogue chain and the effectiveness of the hardening techniques required on the digital blocks. Such techniques included layout with RadHard circuit design and redundancy at the system design (e.g., TMR). The radiation testing of the RadHard accelerometer in its 'final' form (i.e., the current SA1020.a space grade prototype) is planned and the results are expected in Q2 2015

manufacturing process flow) has demonstrated significant performance improvements compared to previous state of the art open-loop accelerometers. These results have been reported herein.

The first full SA0120.a RadHard space grade prototypes have now also been produced and, at the time of writing, are in initial testing. These prototypes integrate the two independent accelerometers in a single ceramic package, along with the radiation hardened ASIC and as such are fully representative of the end product for space applications. The initial test results confirm the good performance of the industrial prototypes. As shown in Table 5, the SA0120.a accelerometer meets the key target specifications and is highly attractive compared to possible alternative products, especially with regard to mass and power.

After completion of the current series of tests, the components will be at TRL level 5. The next steps are intended to be the full evaluation or qualification of the component against ESCC/ECSS standards leading to the off the shelf

availability of the accelerometer component for all space applications.

## References

1. Stauffer, J.-M.: MEMS accelerometers: from market to advanced applications. Position Location and Navigation Symposium, 2004. PLANS 2004, Monterey (2004)
2. Stauffer, J.-M., Dietrich, O., Dutoit, B.: RS9000, a novel MEMS accelerometer family for Mil, Aerospace and Safety Critical Applications, IEEE, ION Position Location and Navigation Symposium (PLANS), Mai 4–6. Indian Wells, California (2010)
3. Zwahlen, P., Dong, Y., Nguyen, A.-M., Rudolf, F., Ullah, P., Ragot, V.: High performance inertial navigation grade sigma-delta. Inertial Sensors and Systems, Karlsruhe (2012)
4. Le Reverend, R.: Device for measuring a force with the aid of a capacitive sensor using charge transfer. US patent US5821421
5. ESA ITT AO/1-6198/09/NL/JD, Accelerometer for IMU feasibility demonstrator, Programme Ref.: TRP T705-032EC
6. IEEE std 1293–1998: IEEE standard specification format guide and test procedure for linear single-axis, nongyroscopic accelerometers, E-ISBN:978-0-7381-6869-2